GREEN SYNTHESIS OF AuNPs FROM THE LEAF EXTRACT OF PROSOPIS FARCTA FOR ANTIBACTERIAL AND ANTI-CANCER APPLICATIONS

O. H. ABDULLAH, A. M. MOHAMMED*
Department of Chemistry, College of Science, University Of Anbar, Ramadi, Iraq

This study involves the synthesis of gold nanoparticles (AuNPs) formed from the *Prosopis farcta* leaf extract. The transmission electron microscope, scanning electron microscope, atomic force microscope, X-ray diffraction, and UV-Visible spectroscopy results all confirmed the characterisation of AuNPs. The in vitro anticancer activity of AuNPs against breast cancer -13 (AMJ-13) and human breast epithelial (HBL) cell lines was investigated, along with its antibacterial activity against gram's positive bacteria, the *Staphylococcus aureus*. AuNPs were found to produce a significant cytotoxic effect on the AMJ-13 cell line, contrary to the HBL cell line, which showed no significant cytotoxicity upon it. The antibacterial activity demonstrated that gram-positive *S. aureus* was affected by AuNPs. These results prove that AuNPs have great potential as anticancer and antibacterial agents and can be used in developing strategies for successful anticancer and antibacterial.

(Received June 8, 2020; Accepted September 23, 2020)

Keywords: Green synthesis, AuNPs, Prosopis farcta, Antibacterial, Anti-cancer

1. Introduction

Cancer, a combination of diseases involving abnormal cell growth with the possibility of spreading to other parts of the body, affects various populations all over the world [1]. Among the types of cancer, breast cancer is a pernicious tumour that appears from the epithelial cells of glandular milk ducts or lobules of the breast [2].

Breast cancer is the second most widespread cancer diagnosis in women globally [3]. In its early stages, breast cancer usually does not cause any pain and may exhibit no noticeable symptoms. As the disease progresses, signs and symptoms can include a lump or thickening in or near the breast; a change in the size or shape of the breast; nipple discharge, tenderness, or retraction (turning inward); and skin irritation, dimpling or scaliness [4].

The risk factors for having breast cancer involve being female, alcohol abuse, older age, having children late in life or not at all, family history of breast cancer, lack of physical exercise, ionising radiation, and hormone replacement therapy [5]. Meanwhile, *Staphylococcus aureus* is a gram-positive, round-shaped bacterium that is a member of the firmicutes and is a common microbiota of the body [6]. Globally, *S. aureus* is one of the most widespread foodborne diseases. It was first recorded whilst investigating a food intoxication resulting from eating cheese, which revealed the presence of micrococci [7]. *Prosopis farcta* is a virtually mutual type that is mainly located in cultivated fields. *P. farcta* is a midget bush (0.4–1 m in height) with extended roots and is broadly utilised in traditional societies as natural alternates or complements to synthetic chemicals [8].

Metal nanoparticles (NPs) are quite interesting for their broad range of applications in nanotechnology and various other fields; these substances are shaped by a group of metal atoms with an oxidation state that is equal to zero [9]. Gold nanoparticles (AuNPs) have a distinct appearance because of their small sizes; moreover, bulk gold has a yellow colour and rigid shape, whilst AuNPs have a wine red colour and unique properties. Therefore, AuNPs have attracted extreme attention due to their applications in many fields [10], such as cancer therapy [11], antibacterial agents [12], probes [13], electronics [14], sensors [15] and diagnosis of diseases [16]. Nanotechnology is used to clarify every technology, which could be used to manipulate matter at the molecular level and make devices, materials, and structures with dimensions of 1–100 nm in at

* Corresponding author: sc.dr.ahmedm.mohammed@uoanbar.edu.iq

least one direction [17]. It also has applications in the food industry [18], medical field [19], electrical transformers [20], agriculture [21], and so on.

The methods for nanomaterial synthesis are classified as one of the two approaches, the top-down approach wherein larger particles are broken down to smaller ones [22], and the bottom-up approach, which generally builds larger structures from the smaller building blocks, namely, atoms [23]. These two approaches could use mechanical [24], chemical [25], physical [26], or biological [27] pathways to form NPs. Among these, the biological approach is the best one for the synthesis of NPs, because it is considered safe for the environment, fast, simple, cheap, and yields good products. In comparison, the chemical and physical methods are considered dangerous for the environment, are expensive and require sophisticated equipment to conduct the synthesis [28,29].

The purpose of this study is to form AuNPs from the *P. farcta* leaf extract and investigate their activity against the AMJ-13 cell line and *S. aureus*.

2. Materials and methods

2.1. Materials

The breast cancer cell line (AMJ-13) was provided by the laboratory unit of Al-Mustansiriyah University, Baghdad, Iraq. Trypsin-EDTA, RPMI-1640, and foetal bovine serum (FBS) were procured from Capricorn (Germany). MTT(3-(4,5-Dimethyl-2-thiazolyl)-2,5-diphenyl-2H-tetrazolium bromide) was bought from Bio-World (USA), whilst dimethyl sulfoxide (DMSO) was obtained from Santacruz Biotech (USA). Muller-Hinton agar was purchased from Hi-Media (India), and Gold(III) Chloride Trihydrate ($HAuCl_4.3H_2O$) was purchased from Sigma-Aldrich (USA). Deionised water (H_2O) was obtained from Chem-Lab (Belgium). Fresh *P. farcta* leaves were collected in November from Saqlawia, Anbar, Iraq, as shown in Fig. 1.

Fig. 1. View of prosopis farcta leaves.

2.2. Methods

2.2.1. Synthesis of the P. farcta leaf extract

The extract was prepared by adding 100 mL of deionised water as a solvent to 2 gm of leaf powder. The mixture was shaken at 200 rpm and heated at 65 ºC for a period of 1 h, after which the resultants were filtered by Whatman filter paper No. 1. A clear brown solution was obtained and kept at 5 ºC.

2.2.2. Synthesis of AuNPs

In this experiment, 10 mL of the aqueous leaf extract was increased to 50 mL by adding an aqueous gold chloride solution (1 mM). The final mixture was shaken at 200 rpm for 20 min at 25 ºC. The colour changed from brown to purplish, which confirmed the formation of AuNPs, as shown in Fig. 2.

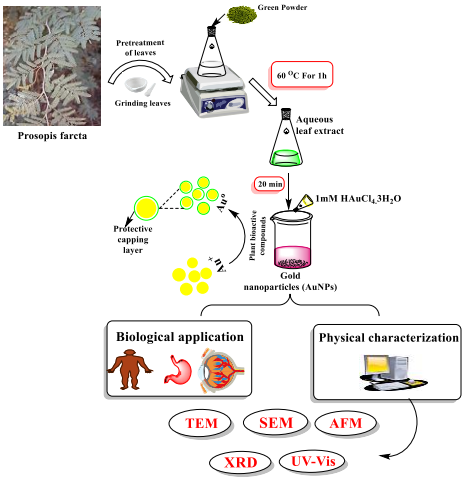

Fig. 2. Synthesis of AuNPs.

2.2.3. Characterisation of AuNPs

The particle size of AuNPs was measured by transmission electron microscope (TEM), scanning electron microscope (SEM), and atomic force microscope (AFM) (SPM-AA3000, Angstrom Advanced Inc., USA). The crystalline size and structure of the NPs were determined through X-ray diffraction (XRD) using an automated diffraction meter (Shimadzu 6000 XRD) with Cu-Kα radiation (λ = 1.5418 Å). The solution of AuNPs was scanned using a UV-Visible spectrophotometer (Shimadzu 1800) to detect the optical properties in the sample.

2.4. Anticancer activity

2.4.1. Cell culture

The AMJ-13 and HBL cells were maintained in RPMI-1640 supplemented with 10% FBS, 100 units/mL penicillin, and 100 µg/mL streptomycin. The cells were passaged using Trypsin-EDTA reseeded at 80% confluence twice a week and incubated at 37 °C [30].

2.4.2. Cytotoxicity determination using MTT assay

To determine the cytotoxic effect of AuNPs, the MTT cell viability assay was conducted using 96-well plates. The cell lines were seeded at 1×10^4 cells/well. After 24 h or once a confluent monolayer was achieved, the cells were treated with tested compounds at different concentrations. Cell viability was measured after 72 h of treatment by removing the medium, adding 28 µL of 2 mg/mL solution of MTT, and then incubating the cells for 2.5 h at 37 °C. After removing the MTT solution, the crystals remaining in the wells were solubilised by the addition of 130 µL of DMSO followed by incubation for 15 min with shaking at 37 °C [31]. The absorbency was determined on a microplate reader at 492 nm. The inhibition rate of cell growth (the percentage of cytotoxicity) was calculated using the following equation:

$$\text{Inhibition rate} = A - B/A * 100,$$

where A is the optical density of control, and B is the optical density of the samples.

To visualise the shape of the cells under an inverted microscope, 200 µL of cell suspensions were seeded in 96-well micro-titration plates at a density of 1×10^4 cells mL^{-1} and incubated for 48 h at 37 °C. Then, the medium was removed and the NPs were added after 24 h. Next, the plates were stained with 50 µL with Crystal violet and incubated at 37 °C for 15 min. The stain was washed gently with tap water until the dye was removed. The cells were observed under an inverted microscope at a 100× magnification microscope and then filmed and photographed with a digital camera.

2.5. Antibacterial activity

2.5.1. Determination of the minimum inhibitory concentration (MIC)

The antibacterial activity of the prepared AuNPs was investigated against gram's positive *S. aureus* bacteria using an agar well diffusion technique. The MIC is defined as the lowest concentration that is able to inhibit bacterial growth. About 20 mL of Muller–Hinton (M–H) was aseptically poured into sterile Petri dishes before culturing. The bacterial species were collected from their stock cultures using a sterile wire loop. After culturing the organisms, 6 mm-diameter wells were bored on the agar plates using a sterile tip [32]. Into the bored wells, different concentrations of the NPs (25, 50, 100, 200) µg/mL were placed. The cultured plates containing the NPs and the test organisms were incubated overnight at 37 °C before measuring and recording the average of the diameter of the produced zones of bacterial inhibition by the respective NP concentrations. The experiments were performed in triplicate.

2.5.2. Statistical analysis

An unpaired t-test was used to make a comparison between the studied groups at a significant p-value of <0.05 [33].

3. Results and discussion

3.1. TEM

The morphological characterisation and particle size of the AuNPs were analysed using TEM. TEM images show the synthesised AuNPs by *P. farcta*. As can be seen in Fig. 3, most of the AuNPs have a spherical shape.

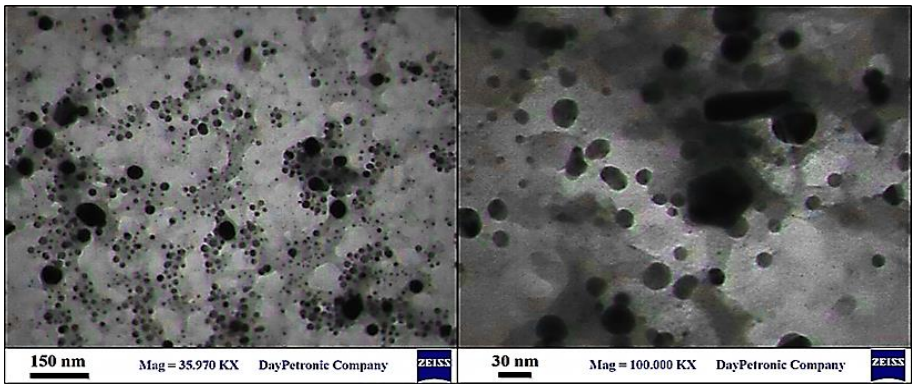

Fig. 3. TEM images of AuNPs.

3.2. SEM

The surface physical morphology of the AuNPs was observed using SEM. The SEM images showed a typical surface of AuNPs prepared from the *P. farcta* leaf extracts with diameters ranging from 23 nm–55 nm, as shown in Fig. 4.

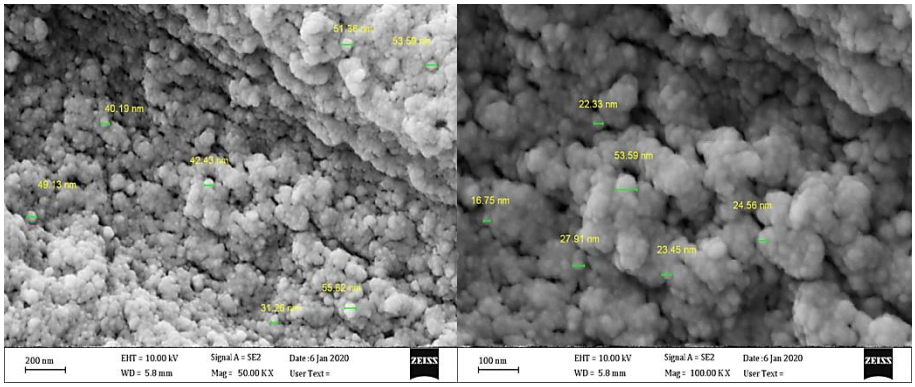

Fig. 4. SEM images of AuNPs.

3.3. AFM

The AFM images of the AuNPs shown in Fig. 5 display the two- and three-dimensional images of the synthesised AuNPs. The images confirmed that the AuNPs had small diameter distribution. Furthermore, the average distribution of the diameter was 59.74 nm.

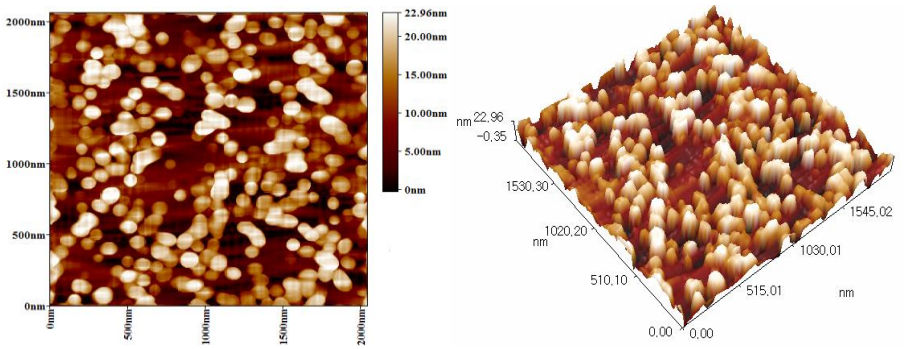

Fig. 5. AFM of two and three dimensional of AuNPs.

3.4. XRD

The XRD images of the sample shown in Fig. 6 were compared with the ICDD card No. 03-065-2870 as the standard reference of the AuNPs. The peaks of diffraction indexed to the (111), (200), (220) and (311) planes confirmed that the observed AuNPs' face centred cubic (fcc) had peaks at $2\theta = 38.18^{o}$, 44.38^{o}, 64.57^{o} and 77.56^{o}, respectively, as shown in all the samples.

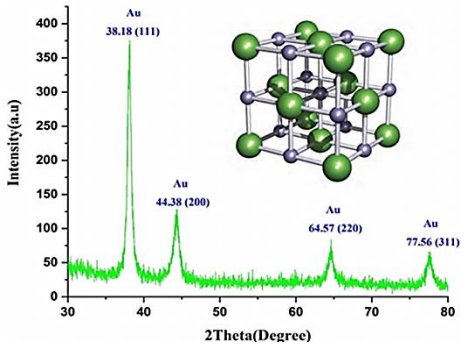

Fig. 6. XRD of AuNPs.

3.5. Measurement of the UV-Visible spectroscopy

The AuNPs were examined using UV-Visible spectroscopy. As shown in Fig. 7, the electronic spectrum of the synthesised AuNPs showed a broad peak at 532 nm, which displayed the formation of Au-NPs. The size of the AuNPs was influenced by surface plasmon resonance as can be seen in the plasmon bandwidth.

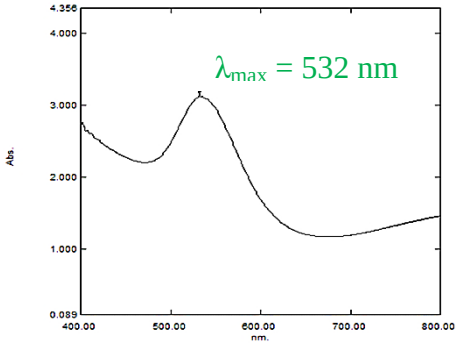

Fig. 7. UV-Visible spectrum of AuNPs.

3.6. Anticancer activity

The anticancer activity of AuNPs was studied using the MTT assay. MTT assay is a colorimetric assay that analyses the color changes via the metabolic activity of active cells. The cytotoxicity of AuNPs on the viability of the human breast cancer (AMJ-13) and HBL cell lines was studied for 72 h. The results are shown in Fig. 8. The results displayed an important inhibition of the AMJ-13 proliferation after 72 h: the cell proliferation was significantly reduced compared with the untreated control cells. After 72 h of treatment with AuNPs at the concentrations of 6.25, 12.5, 25, 50, and 100 µM/mL, significant cytotoxicity against the AMJ-13 cell line was observed: AuNPs killed >70 % of the cells. In comparison, AuNPs showed no significant effect on the HBL cells. Furthermore, the AMJ-13 cell line was more sensitive to AuNPs than the HBL cells, indicating that AuNPs had a selective effect towards the cancer cell lines. Hence, the effect of AuNPs depended on the type of cells.

The results suggest that AuNPs are a potential source of efficient antiproliferative and cytotoxic materials. By using an inverted phase-contrast microscope, the apoptogenic advantage of AuNPs was also examined through the morphological changes on the AMJ-13 cell line. As shown in Fig. 9, the control, untreated cells preserved their actual morphology and were mostly stuck to the tissue plate. Treatment with AuNPs showed morphological variations and high antiproliferation activities on the cells after 72 h. In comparison, our results displayed no morphological changes on the HBL cells after treatment with AuNPs at the same concentration (Fig. 9). This suggests that the NPs have potential for in vivo applications [34].

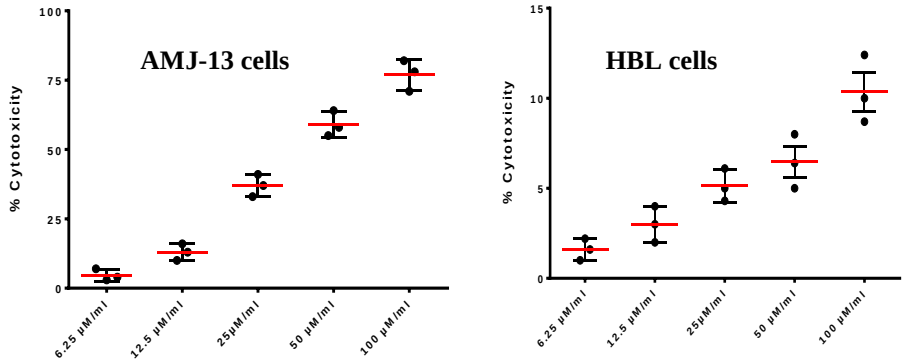

*Fig. 8. Cytotoxicity of AuNPs on AMJ-13 and HBL cell line. The values represent the Mean ± S.E. **P<0.01, ***P<0.001.*

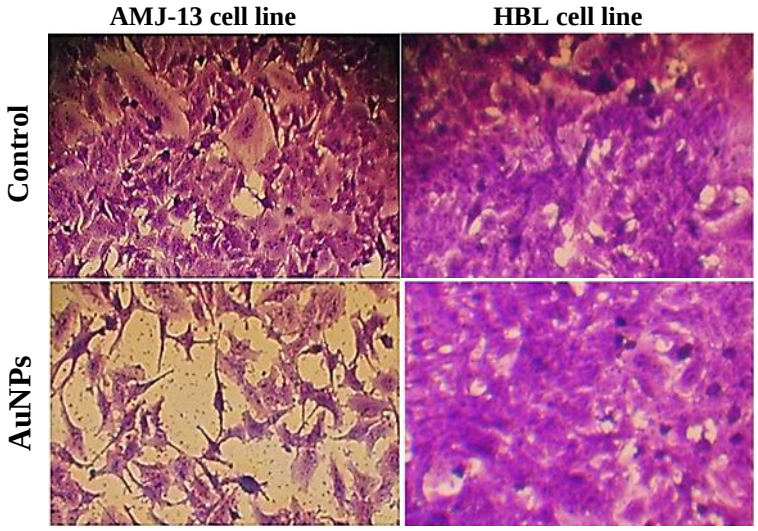

Fig. 9. Antiproliferative activity of AuNPs on AMJ-13 and HBL cell line

3.7. Antibacterial activity

The antibacterial activity of AuNPs was assessed using the agar well diffusion technique. In the present study, standard strain S. aureus was used. The zone of inhibition of AuNPs was also measured, as shown in Fig. 10. The antibacterial activities against S. aureus of AuNPs at concentrations of 20, 10, 5, and 2.5 mM/mL showed inhibition zones of 11, 13.92, 17.60, and 19.85 mm, respectively. Hence, AuNPs displayed an increase in inhibition zone with a decrease of sample concentration. This indicates that the diffusion in particles with less concentration is probably more likely than that in the higher concentration sample. This also demonstrates that the fewer particles found in the sample have greater exposure to more colonies of cell congregation. Fewer concentrations of the NPs exhibited a larger zone of inhibition. However, the results contradict earlier findings, which stated that antibacterial activity is increased when the concentration of the sample is increased [35]. This can be observed by shrinking zone of inhibition on the petri dish.

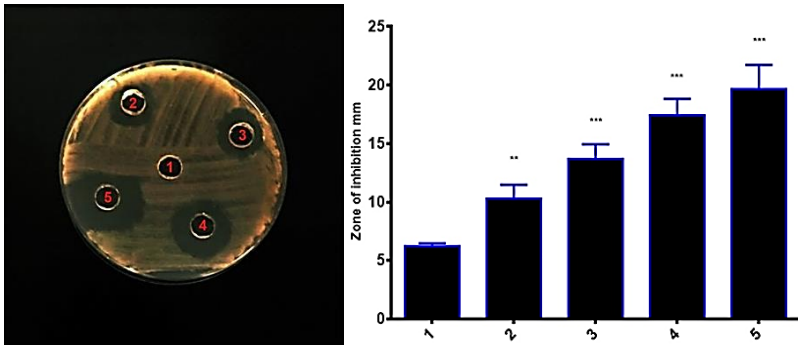

*Fig.10. Antibacterial activity of AuNPs against S. aureus. 1. Negative control (DMSO) 2. Concentration 20 mM/mL 3. Concentration 10 mM/mL4. Concentration 5 mM/mL 5. Concentration 2.5mM/mL. The value are shown as the mean±SEM. **p<0.01, and ***p<0.001.*

4. Conclusion

The study investigated the efficiency of the biological pathway using *P. farcta* leaf extracts to obtain AuNPs with a small diameter. This approach represents a simple, economical, and cost-effective way of producing NPs with less time and less energy requirement. Moreover, AuNPs were found to have huge potential as anticancer and antimicrobial delivery systems.

Furthermore, the results suggest that AuNPs should be further investigated for potential biomedical applications.

References

[1] J. Ferlay, I. Soerjomataram, R. Dikshit, S. Eser, C. Mathers, M. Rebelo, F. Bray, International Journal of Cancer **136**(5), E359 (2015).
[2] M. Capelan, N. M. L. Battisti, A. McLoughlin, V. Maidens, N. Snuggs, P. Slyk, A. Ring, British journal of cancer **117**(8), 1113 (2017).
[3] A. V. Lee, S. Oesterreich, N. E. Davidson, JNCI: Journal of The National Cancer Institute **107**(7), 1 (2015).
[4] J. Polivka, I. Altun, O. Golubnitschaja, EPMA Journal **9**(1), 1 (2018).
[5] M. Mustafa, A. Nornazirah, F. Salih, E. Illzam, M. Suleiman, A. Sharifa, IOSR Journal of Dental and Medical Sciences **15**(08), 73 (2016).
[6] J. H. Kim, S. Y. Han, J. H. Kwon, D. S. Lee, Asian Pacific Journal of Tropical Medicine **13**(1), 38 (2020).
[7] J. A. Hennekinne, M. L. De Buyser, S. Dragacci, FEMS Microbiology Reviews **36**(4), 815 (2012).
[8] I. H. Mohammed, E. S. Kakey, Iraqi Journal of Veterinary Sciences **34**(1), 45 (2020).
[9] S. Guo, E. Wang, Nano Today **6**(3)**,** 240 (2011).
[10] J. Lu, Y. Li, Y. Han, Y. Liu, J. Gao, Applied Optics **57**(19), 5268 (2018).
[11] M. Vairavel, E. Devaraj, R. Shanmugam, Environmental Science and Pollution Research **27**, 8166 (2020).
[12] H. Dang, D. Fawcett, G. E. J. Poinern, International Journal of Research in Medical Sciences **7**(4), 221 (2019).
[13] D. J. Hamilton, Y. Cai, R. Kaur, G. W. Marquart, M. R. Mackiewicz, S. M. Reed, Lipid coated gold nanoparticles as probes for membrane binding. In chemical and synthetic approaches in membrane biology, Humana Press, New York, NY, 1 (2016).
[14] D. Huang, F. Liao, S. Molesa, D. Redinger, V. Subramanian, Journal of the Electrochemical Society **150**(7), G412 (2003).
[15] S. Zeng, K. T. Yong, I. Roy, X. Q. Dinh, X. Yu, F. Luan, Plasmonics **6**(3), 491 (2011).
[16] A. J. Mieszawska, W. J. Mulder, Z. A. Fayad, D. P. Cormode, Molecular pharmaceutics **10**(3), 831 (2013).
[17] M. Ferrari, Nature reviews cancer **5**(3), 161 (2005).
[18] E. Inshakova, O. Inshakov, In MATEC Web of Conferences EDP Sciences **129**, 2013 7).
[19] C. G. Yao, P. N. Martins, Transplantation **104**(4), 682 (2020).
[20] A. Thabet, M. Allam, S. A. Shaaban, Electric Power Components and Systems **47**(4-5), 420 (2019).
[21] N. Mitter, K. Hussey, Nature nanotechnology **14**(6), 508 (2019).
[22] M. Zensich, T. Jaumann, G. M. Morales, L. Giebeler, C. A. Barbero, J. Balach, Electrochimica Acta **296**, 243 (2019).
[23] A. Farag, L. Lu, H. R. Roth, J. Liu, E. Turkbey, R. M. Summers, IEEE Transactions on Image Processing **26**(1), 386 (2016).
[24] J. J. Li, Y. X. Hu, M. C. Liu, L. B. Kong, Y. M. Hu, W. Han, L. Kang, Journal of Alloys and Compounds **656**, 138 (2016).
[25] S. Pradhan, R. Das, S. Biswas, D. K. Das, R. Bhar, R. Bandyopadhyay, P. Pramanik, Electrochimica Acta **238**, 185 (2017).
[26] C. Yang, X. Yan, H. Guo, G. Fu, Biosensors and Bioelectronics **75**, 129 (2016).
[27] I. Hussain, N. B. Singh, A. Singh, H. Singh, S. C. Singh, Biotechnology Letters **38**(4), 545 (2016).
[28] S. Pradhan, R. Das, S. Biswas, D. K. Das, R. Bhar, R. Bandyopadhyay, P. Pramanik, Electrochimica Acta **238**, 185 (2017).

[29] D. M. Liu, J. Chen, Y. P. Shi, Analytica Chimica Acta **1006**, 90 (2018).
[30] Z. Ali, M. Jabir, A. Al-Shammari, Research Journal of Biotechnology **14**, 79 (2019).
[31] S. H. Ali, G. M. Sulaiman, M. M. Al-Halbosiy, M. S. Jabir, A. H. Hameed, Artificial Cells, Nanomedicine, and Biotechnology **47**(1), 378 (2019).
[32] K. S. Khashan, M. S. Jabir, F. A. Abdulameer, Materials Research Express **5**(3), 035003 (2018).
[33] S. Albukhaty, H. Naderi-Manesh, T. Tiraihi, J. M. Sakhi, Artificial Cells, Nanomedicine, and Biotechnology **46**(sup 3), S125 (2018).
[34] H. Nosrati, M. Salehiabar, E. Attari, S. Davaran, H. Danafar, H. K. Manjili, Applied Organometallic Chemistry **32**(2), e4069 (2018).
[35] A. M. Mohammed, W. M. Saud, M. M. Ali, Digest Journal of Nanomaterials and Biostructures **15**(1), 175 (2020).